BUCKLING ANALYSIS OF CANTILEVER TWISTED FGM PLATE

A THESIS SUBMITTED IN PARTIAL FULFILMENT

OF THE REQUIREMENTS FOR THE DEGREE OF

Master of Technology

In

Structural Engineering

Submitted By

INDRAJEETH M S

Roll No. : 213CE2066

DEPARTMENT OF CIVIL ENGINEERING

NATIONAL INSTITUTE OF TECHNOLOGY, ROURKELA

ORISSA, INDIA- 769008

MAY 2015

BUCKLING ANALYSIS OF CANTILEVER TWISTED FGM PLATE

A THESIS SUBMITTED IN PARTIAL FULFILMENT

OF THE REQUIREMENTS FOR THE DEGREE OF

Master of Technology

In

Structural Engineering

Submitted By

INDRAJEETH M S

Roll No. : 213CE2066

Guided by

Prof. A. V. ASHA

DEPARTMENT OF CIVIL ENGINEERING

NATIONAL INSTITUTE OF TECHNOLOGY, ROURKELA

ORISSA, INDIA – 769008

MAY 2015

DEPARTMENT OF CIVIL ENGINEERING

NATIONAL INSTITUTE OF TECHNOLOGY, ROURKELA

ODISHA, INDIA

CERTIFICATE

This is to certify that the thesis entitled "**BUCKLING ANALYSIS OF CANTILVER TWISTED FGM PLATE**", submitted by **INDRAJEETH M S** bearing **Roll no. 213CE2066** in partial fulfilment of the requirements for the award of ***Master of Technology*** in the Department of Civil Engineering, National Institute of Technology, Rourkela is an authentic work carried out by him under my supervision and guidance.

To the best of my knowledge, the matter embodied in the thesis has not been submitted to any other university/Institute for the award of any Degree or Diploma.

Place: Rourkela

Date: 01 June 2015

Prof. A. V. ASHA

Civil Engineering Department

National Institute of Technology, Rourkela

DEPARTMENT OF CIVIL ENGINEERING

NATIONAL INSTITUTE OF TECHNOLOGY

ROURKELA 769008

A C K N O W L E D G E M E N T

It gives me immense pleasure to express my deep sense of gratitude to my supervisor **Prof. A. V. Asha** for her invaluable guidance, motivation, constant inspiration and above all for her ever co-operating attitude that enabled me to bring up this thesis to the present form.

I express my sincere thanks to the Director, **Prof. S. K. Sarangi,** National Institute of Technology, Rourkela for motivating me in this endeavor and providing me the necessary facilities for this study.

I am extremely thankful to **Prof. S. K. SAHU**, Head of the Department of Civil Engineering for providing all help and advice during the course of this work.

I am greatly thankful to all the staff members of the department. Many friends and my classmates have helped me stay sane through these difficult years. Their support and care helped me overcome setbacks and stay focused on my study. I greatly value their friendship and I deeply appreciate their belief in me.

Last but not the least I would like to thank **my parents**, who taught me the value of hard work and encouraged me in all my endeavours.

Place: Rourkela
Date**:** 01 June 2015

INDRAJEETH M S
M. Tech., Roll No: 213CE2066
Specialization: Structural Engineering
Department of Civil Engineering
National Institute of Technology, Rourkela

ABSTRACT

The demand and application of composites are increasing nowadays. Composite materials in the form of plate or plate-like structures are widely used in wind turbine blades and ship building due to its high specific strength and stiffness. For high thermal applications, Functionally Graded Materials (FGM) are used in preference to laminated composites because of its good performance in the thermal field. The pre-twisted cantilever plates have major use in turbine blades, fan blades, compressor blades, chopper blades, marine propellers and chiefly in gas turbines. These structures are often subjected to thermal environments, and hence FGMs are a good alternative to metal plates.

The present work deals with the study of buckling analysis of cantilever twisted functionally graded material plates. The analysis is done by using ANSYS, and the results are validated using ABAQUS. A SHELL-281 element having six degrees of freedom per node is employed in ANSYS. The functionally graded material plate with a uniform variation of the material property through the thickness is estimated as a laminated section containing number of layers, and each layer is taken as isotropic. The power law is used to determine material properties in each layer. From convergence studies, ten by ten mesh and twelve number of layers are found to give good accuracy. Buckling behavior of cantilever twisted FGM plate for the various parameters like twist angle, side to thickness ratio, aspect ratio and gradient index are studied.

KEYWORDS: Functionally graded materials, Pre-twist, Buckling.

CONTENTS

LIST OF FIGURES

LIST OF TABLES

NOMENCLATURE

The principal symbols used in this thesis are presented for reference. Every symbol is used for different meanings depending on the context and defined in the text as they occur.

a, b	Length and width of twisted panel
a/ b	Aspect ratio
H	Thickness of Plate
b/ h	Width to thickness ratio
Φ	Angle of twist
N	Gradient index
E	Modulii of elasticity
G	Shear Modulii
N	Poisson's ratio
K	Shear correction factor
k_x, k_y, k_{xy}	Bending strains
Mx, My, Mxy	Moment resultants of the twisted panel
[N]	Shape function matrix
N_x, N_y, N_{xy}	In-plane stress resultants of the twisted panel
N_x^0, N_y^0, N_{xy}^0	External loading in the X and Y directions respectively
A_{ij}, B_{ij}, D_{ij} *and* S_{ij}	Extensional, bending-stretching coupling, bending and transverse shear stiffnesses
dx, dy	Element length in x and y-direction
dV	Volume of the element
Q_x , Q_y	Shearing forces
R_x, R_y, R_{xy}	Radii of curvature of shell in x and y directions and radius of twist
u, v, w	Displacement components in the x, y, z directions at any point
u_o, v_o, w_o	Displacement components in the x, y, z directions at the mid-surface
[P]	Mass density parameters

Q	Vector of degrees of freedom
x_i, y_i	Cartesian nodal coordinates
Γ	Shear strains
σ_x σ_y τ_{xy}	Stresses at a point
σ_x^0, σ_y^0 and σ_{xy}^0	In-plane stresses due to external load
τ_{xy}, τ_{xz}, τ_{yz}	Shear stresses in xy, xz and yz planes respectively
ε_x, ε_y, γ_{xy}	Strains at a point
ε_{xnl}, ε_{ynl}, ε_{xynl}	Non-linear strain components
θ_x, θ_y	Rotations of the midsurface normal about x- and y- axes respectively
N_x	Critical Buckling load
Λ	Non-dimensional buckling load
$(\rho)_k$	Mass density of kth layer from mid-plane
P	Mass density of the material
$\partial/\partial x$,$\partial/\partial y$	Partial derivatives with respect to x and y

Chapter 1

INTRODUCTION

CHAPTER 1

INTRODUCTION

1.1 Introduction

A composite material is a structural material made from two or more constituent materials with significantly distinct physical or chemical properties, which when fused produce a material with characteristics unlike that of the individual components. The main advantage of a composite material is that they are light as well as strong. Functionally Graded Materials (FGM) are a set of composites that exhibit a uniform change of material properties from one face to another and hence eliminate the stress concentration, normally encountered in laminated composites. The characteristics of these FGM's are the ability to yield a new composite material with uniform composition variation from thermal resistant ceramics to fracture resistant metals. The FGM concept originated in the year 1984 in Japan during a space research program. This program envisaged the manufacture of a temperature resistant material to resist a temperature of 2000 Kelvin and a temperature gradient of 1000 Kelvin having a thickness below 10mm. The structural component of an FGM can be characterized by the material constituents. It shows the rate of change of material properties. The gradient index governs the chemical configuration, geometric configuration and physical state of FGM. Primarily FGM involves two material mixtures in which material configuration changes from one surface to another. Variation of porosity from one face to another face also yields functionally graded material. A steady rise in porosity builds impact resistance, thermal resistance, and low density. These FGM's have significant applications in civil and mechanical structures including thermal structures like

Rocket heat shield, heat exchanger tubes, wear resistance linings, thermos-elastic generators, diesel, and turbine engines, etc.

The major applications of pre-twisted cantilever panels are in turbine blades, fan blades, compressor blades, chopper blades, marine propellers and chiefly in gas turbines. Nowadays, in research field the twisted plates have become key structural units. Because of the use of twisted panels in turbomachinery, aerospace and aeronautical industries, it is necessary to understand both vibration and buckling characteristics of the pre-twisted panels.

1.2 Importance of Present study

Composite materials in the form of plate or plate-like structures are widely used in wind turbine blades and a certain type of ships, particularly naval ships. Functionally graded material plates are finding increasing application in many structures, especially where the temperature is high. The plates are also subjected to loads due to fluid or hydrodynamic loading. Thus, understanding and proper application of composite materials have helped to control the lifetime and stability of these constructions. Hence, the buckling analysis plays a crucial role in the design context. From the literature review, it shows that there is plenty of work done in the area of flat FGM plates. However, no work has been done on the buckling behavior of twisted FG material panels and hence the present study.

1.3 Outline of the present work

The present work consists of the studies made on the buckling behavior of twisted FG material plates. The influence of different parameters like twist angle, width to thickness ratio, aspect ratio, and material gradient index are studied.

The outline of this thesis is divided into five chapters.

Chapter 1 consists of brief introduction on FGM, importance of present study and the outline of present work.

Chapter 2 gives literature reviews on previous studies related to the present study and also the objectives of the present studies are explained.

In chapter 3, the theoretical formulations are presented. The methodology used for the modeling of the functionally graded plate is also discussed.

Chapter 4 consists of convergence studies, comparison studies and the studies of buckling behavior of cantilever twisted FGM plate for the various parameters like twist angle, aspect ratio, side to thickness ratio and gradient index.

Chapter 5 contains the conclusions made from the present work and its scope in future work.

Chapter 2

LITERATURE REVIEW

CHAPTER 2

LITERATURE REVIEW

2.1 Literature review

Reddy (2000) [14] presented the study of FG plates using third-order shear deformation theory. The material distribution and modulus of elasticity along thickness were assumed to vary based on power-law distribution. The results showed the influence of volume fraction and modular ratio on deflections and transverse shear stresses.

Javaheri and Eslami (2002) [6] derived equilibrium equations and stability equations of rectangular FG plate using higher-order shear deformation theory (HSDT) subjected to thermal load. The derived equation was found to be identical to the stability and equilibrium equations of laminated composite plates.

Buckling behaviour of FG plates with geometrical imperfections under in-plane compressive loading was studied by *Shariat et al. (2005)* [17]. The Classical Plate Theory was used for the derivation of equations of equilibrium, stability, and compatibility. From their study, it was concluded that the imperfect FG plate has greater buckling load than that of the perfect plate. As the imperfection increases, the critical buckling load also increases which can be reduced by increasing power law index.

Yang et al. (2006) [21] presented the sensitivity of post-buckling behaviour of FG material plates to initial geometric imperfections such as local type, global type, and sine type imperfections in general modes. The formulations used were based on Reddy's Higher order Shear Deformation

Theory and von Karman type geometric non-linearity. The results showed that the post-buckling strength was comparatively insensitive to sine mode and global imperfections. However, it was highly sensitive to local imperfections that were situated at the center of the plate. They also concluded that the post-buckling curves were lowered by an increase in the side to thickness ratio, gradient index and aspect ratio. They observed that these curves were less sensitive to imperfection sensitivity of the post-buckling reaction of the plate.

Shariat and Eslami (2007) [18] used third-order shear deformation theory for the analysis of buckling of thick rectangular FG plates under various mechanical and thermal loads. The mechanical loadings were uniaxial compression, biaxial compression and biaxial compression with tension. The thermal loads were a uniform rise in temperature and non-linear rise in temperature. It was concluded that for the thick plates, the critical buckling load was over-predicted by the classical plate theory and in order to have precise buckling load values it was recommended that the third-order shear deformation theory was necessary.

Prakash et al. (2008) [13] presented post-buckling behaviour of FGM skew plates based on shear deformable finite element approach under thermal loads. The temperature field was assumed to vary along the thickness direction only and to be constant over the plate surface. The thermal load carrying capacity increased with increasing skew angle.

Mahadavian (2009) [7] considered simply supported rectangular plates under non-uniform compression loads for the analysis of buckling of FG plate and derived equations of equilibrium and stability for the same and also achieved results for FGM sample. In addition, he also studied the buckling coefficient caused by the outcome of power law index.

Zhao et al. (2009) [23] used FSDT along with the element free *kp*-Ritz method for the buckling analysis of FG plates under thermal and mechanical loading. The buckling analysis of FG plate with arbitrary geometry including plates with square and circular holes at the centre was investigated. In results, it was stated that the hole size influenced buckling load and buckling mode of a plate significantly.

Mohammadi et al. (2010) [10] presented Levy solution for the buckling analysis of FG plates. The plate was assumed to be simply supported along two edges face to face and on the other edges to have arbitrary boundary conditions. It was concluded that the critical buckling load decreased with the increase of power of FGM.

The thermal buckling analysis of FG plates using sinusoidal shear deformation plate theory (SPT) was presented by *Zenkour et al. (2010)* [2]. Various types of thermal loads were considered for the buckling analysis of simply supported rectangular FG plate. The results presented for SPT was compared with other theories to demonstrate its importance and accuracy.

Zenkour and Sobhy (2010) [24] used the sinusoidal SPT to study the thermal buckling of FGM sandwich plates. They concluded that the critical buckling temperature decreased with increase in core thickness of the plate.

Naderi and Saidi (2011) [12] presented an exact analytical solution for buckling of moderately thick FG plates resting on Winkler elastic foundations. The first order shear deformation theory was considered for developing equilibrium equations. The thickness of plate has less effect on the stability of FG plates resting on the elastic foundation than that of plates without elastic foundation.

The buckling analysis of thin rectangular FGM plate under thermal loads using higher order deformation theory was studied by *Raki et al. (2012)* [11]. It was concluded that the higher order deformation theory predicts buckling behaviour accurately.

Saha and Maiti (2012) [15] investigated the buckling of simply supported FGM plates loaded with constant and linearly varying in-plane compressive load. The HSDT was used to study the effect of shear deformation in the case of constant compression loading and classical plate theory as in the case of linearly varying load. The buckling results of FGM plate were compared with the corresponding isotropic plate and it was found that their ratios were more or less independent of loading parameter, aspect ratio and width-thickness ratio and were functions of only material gradient index.

Latifi et al. (2013) [9] used Fourier series expansion for the buckling analysis of FG material plates. Various edge conditions were considered. Here the stability equations were derived from the classical plate theory and found accuracy in the proposed approach in the results of buckling analysis.

Reddy et al. (2013) [20] used HSDT for the solutions of buckling analysis of simply supported FG plates and concluded that the theory was precise and efficient in predicting the buckling behaviour of FG plates.

Sarrami-Foroushani et al. (2013) [19] used finite strip method to analyse the buckling of FG stiffened and unstiffened plates based on CPT. the stiffness and stability matrices were obtained by using the principle of minimum total potential energy. Various loading types were considered to find critical stresses of rectangular FG plates using the matrix Eigenvalue problem technique.

Bhandari and Purohit (2014) [8] analysed FGM plate under transverse load for various end conditions. The volume fraction distribution was considered based on power law, exponential and sigmoidal distribution. The bending response of E-FGM was found to be nearer to the behaviour of P-FGM.

Zhang et al. (2014) [22] studied the buckling behavior of FGM plates under mechanical and thermal loads using the Kriging meshless method. The discrete Eigenvalue equations were established in terms of first order shear deformation theory and local Petrov-Galerkin formulation. The Kriging technique was used to construct shape function to approximate the displacement fields. Convergence studies were made to depict the method presented was effective and accurate.

2.2 Objective of present study

From the literature review, we can observe there has been plenty of work done on buckling of flat FGM plates. However, no work is done on twisted FGM plate. This thesis deals with the study of buckling of cantilever twisted FG material plate. The study involves the modelling of twisted FGM plate using shell element and solving the buckling problem using finite element method software ANSYS and then to validate results in ABAQUS. The effect of several factors like twist angle, aspect ratio, side to thickness ratio and material gradient index are studied.

Chapter 3

FORMULATION

CHAPTER 3

FORMULATION

3.1 Characteristics of Twisted plate

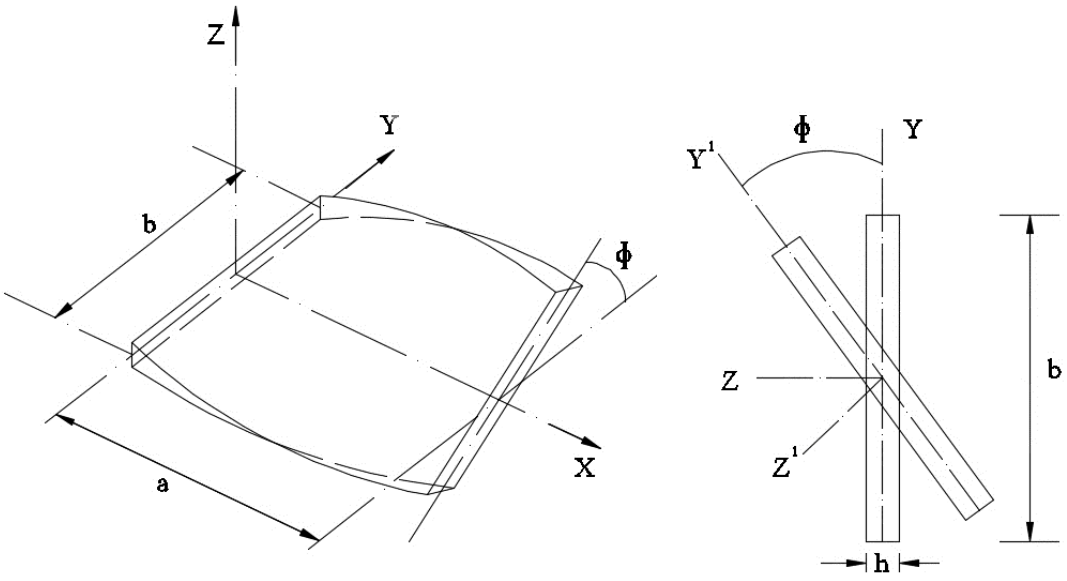

Figure 3. 1: Laminated twisted plate

The Figure 3. 1: Laminated twisted plate illustrates a twisted FGM plate.

Here, Φ = Twist angle.

a and b = length and width of the plate respectively.

h = Thickness of the plate.

3.2 Governing Differential Equations

Consider an element of pretwisted panel with radius of curvatures R_x in x-direction and R_y in y-direction shown in Figure 3. 2. The internal forces acting on the element are membrane forces (N_x , N_y and N_{xy}), shearing forces (Q_x and Q_y) and the moment resultants (M_x , M_y and M_{xy}).

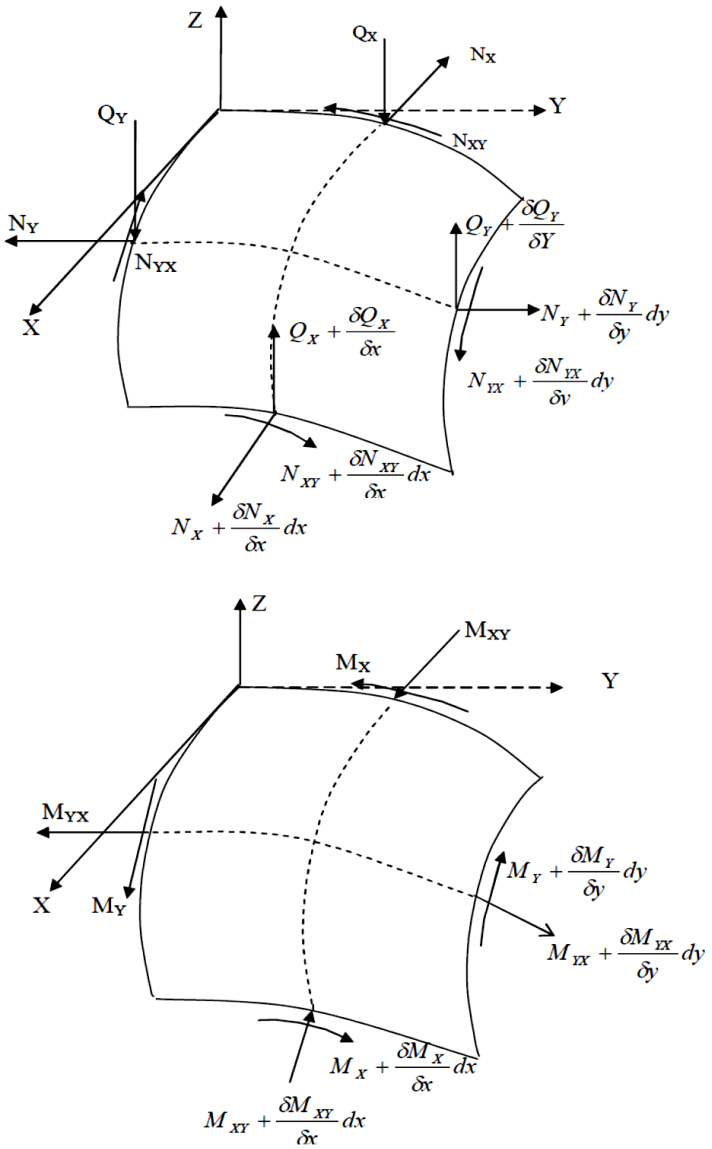

Figure 3. 2: Twisted shell panel element

The governing differential equations of equilibrium for shear deformable doubly curved pre-twisted panel is given as (Sahu and Datta [16], Chandrashekhara [4]):

$$\frac{\partial N_x}{\partial x}+\frac{\partial N_{xy}}{\partial y}-\frac{1}{2}\left(\frac{1}{R_x}-\frac{1}{R_y}\right)\frac{\partial M_{xy}}{\partial y}+\frac{Q_x}{R_x}+\frac{Q_y}{R_{xy}}=P_1\frac{\partial^2 u}{\partial t^2}+P_2\frac{\partial^2 \theta_x}{\partial t^2}$$

$$\frac{\partial N_{xy}}{\partial x}+\frac{\partial N_y}{\partial y}-\frac{1}{2}\left(\frac{1}{R_y}-\frac{1}{R_x}\right)\frac{\partial M_{xy}}{\partial x}+\frac{Q_y}{R_y}+\frac{Q_x}{R_{xy}}=P_1\frac{\partial^2 v}{\partial t^2}+P_2\frac{\partial^2 \theta_y}{\partial t^2}$$

$$\frac{\partial Q_x}{\partial x}+\frac{\partial Q_y}{\partial y}-\frac{N_x}{R_x}-\frac{N_x}{R_y}-2\frac{N_{xy}}{R_{xy}}+N_x^0\frac{\partial^2 w}{\partial x^2}+N_y^0\frac{\partial^2 w}{\partial y^2}=P_1\frac{\partial^2 w}{\partial t^2} \qquad 3.01$$

$$\frac{\partial M_x}{\partial x}+\frac{\partial M_{xy}}{\partial y}-Q_x=P_1\frac{\partial^2 \theta_x}{\partial t^2}+P_2\frac{\partial^2 u}{\partial t^2}$$

$$\frac{\partial M_{xy}}{\partial x}+\frac{\partial M_y}{\partial y}-Q_y=P_1\frac{\partial^2 \theta_y}{\partial t^2}+P_2\frac{\partial^2 v}{\partial t^2}$$

Where,

N_x^0 - External loading in x-direction and N_y^0 - External loading in y-direction.

R_x - Radius of curvature in x-direction, R_y - Radius of curvature in y-direction and

R_{xy} - Radius of twist.

$$\left(P_1,P_2,P_3\right)=\sum_{k=1}^{n}\int_{Z_{k-1}}^{Z_k}\left(\rho\right)_k\left(1,\mathrm{z},\mathrm{z}^2\right)dz \qquad 3.02$$

Here,

n= number of layers of the FGM twisted panel.

$\left(\rho\right)_k$ = mass density at kth layer .

3.3 Constitutive Relations

The linear constitutive relations are given by,

$$\begin{Bmatrix} \sigma_x \\ \sigma_y \\ \tau_{xy} \\ \tau_{xz} \\ \tau_{yz} \end{Bmatrix} = \begin{bmatrix} Q_{11} & Q_{12} & 0 & 0 & 0 \\ Q_{12} & Q_{11} & 0 & 0 & 0 \\ 0 & 0 & Q_{44} & 0 & 0 \\ 0 & 0 & 0 & Q_{55} & 0 \\ 0 & 0 & 0 & 0 & Q_{66} \end{bmatrix} \begin{Bmatrix} \varepsilon_x \\ \varepsilon_y \\ \gamma_{xy} \\ \gamma_{xy} \\ \gamma_{xy} \end{Bmatrix} \quad 3.03$$

Where, $Q_{11} = \dfrac{E}{\left(1-\nu^2\right)}$ 3.04

$$Q_{12} = \frac{\nu E}{\left(1-\nu^2\right)} \quad 3.05$$

$$Q_{44} = \frac{E}{2(1+\nu)} = Q_{55} = Q_{66} \quad 3.06$$

For the FGM plates, the constitutive relations are expressed as:

$$\{F\} = [D]\{\varepsilon\} \quad 3.07$$

Where, $[D] = \begin{bmatrix} A_{11} & A_{12} & A_{16} & B_{11} & B_{12} & B_{16} & 0 & 0 \\ A_{21} & A_{22} & A_{26} & B_{21} & B_{22} & B_{26} & 0 & 0 \\ A_{16} & A_{26} & A_{66} & B_{16} & B_{26} & B_{66} & 0 & 0 \\ B_{11} & B_{12} & B_{16} & D_{11} & D_{12} & D_{16} & 0 & 0 \\ B_{21} & B_{22} & B_{26} & D_{12} & D_{22} & D_{26} & 0 & 0 \\ B_{16} & B_{26} & B_{66} & D_{16} & D_{26} & D_{66} & 0 & 0 \\ 0 & 0 & 0 & 0 & 0 & 0 & S_{44} & S_{45} \\ 0 & 0 & 0 & 0 & 0 & 0 & S_{45} & S_{66} \end{bmatrix}$, $\{F\} = \begin{Bmatrix} N_x \\ N_y \\ N_{xy} \\ M_x \\ M_y \\ M_{xy} \\ Q_x \\ Q_y \end{Bmatrix}$, $\{\varepsilon\} = \begin{Bmatrix} \varepsilon_x \\ \varepsilon_y \\ \gamma_{xy} \\ K_x \\ K_y \\ K_{xy} \\ \varphi_x \\ \varphi_y \end{Bmatrix}$

Coefficients of stiffness are expressed as:

$$\left(A_{i,j}, \mathrm{B}_{i,j}, \mathrm{D}_{i,j}\right) = \sum_{k=1}^{n} \left[Q_{ij}\right]_k \left(1, z, z^2\right) dz \qquad \text{For (i, j=1, 2, 6)} \qquad 3.08$$

$$S_{ij} = k \sum_{k=1}^{n} \int_{z_{k-1}}^{z_k} \left[Q_{ij}\right]_k dz$$

The forces and moment resultants can be obtained by integrating stresses over thickness.

$$\begin{bmatrix} N_x \\ N_y \\ N_{xy} \\ M_x \\ M_y \\ M_{xy} \\ Q_x \\ Q_y \end{bmatrix} = \int_{-h/2}^{h/2} \begin{Bmatrix} \sigma_x \\ \sigma_y \\ \tau_{xy} \\ \sigma_x z \\ \sigma_y z \\ \tau_{xy} z \\ \tau_{xz} \\ \tau_{yz} \end{Bmatrix} dz \qquad 3.09$$

Where,

σ_x - Normal stress in x-direction, σ_y - normal stress in y-direction.

τ_{xy}, τ_{yz} and τ_{xz} are shear stresses in xy, yz and xz planes respectively.

3.4 Strain Displacement Relations

The total strain is considered in two parts namely linear strain and non-linear strain. The element stiffness matrix is derived using linear strain part and the geometric stiffness part is derived by using nonlinear strain part. The total strain is expressed as

$$\xi = \xi_l + \xi_{nl}$$

The linear strain part for a twisted shell element is,

$$\xi_{xl} = \frac{\partial u}{\partial x} + \frac{w}{R_x} + z k_x$$

$$\xi_{yl} = \frac{\partial v}{\partial y} + \frac{w}{R_y} + zk_y$$

$$\gamma_{xyl} = \frac{\partial u}{\partial y} + \frac{\partial v}{\partial x} + \frac{2w}{R_{xy}} + zk_{xy} \qquad 3.10$$

$$\gamma_{yzl} = \frac{\partial w}{\partial y} + \theta_y - \frac{v}{R_y} - \frac{u}{R_{xy}}$$

$$\gamma_{xzl} = \frac{\partial w}{\partial x} + \theta_x - \frac{u}{R_x} - \frac{v}{R_{xy}}$$

Bending components are given by,

$$k_x = \frac{\partial \theta_x}{\partial x} \qquad k_y = \frac{\partial \theta_y}{\partial y}$$

$$k_{xy} = \frac{\partial \theta_x}{\partial y} + \frac{\partial \theta_y}{\partial x} + \frac{1}{2}\left(\frac{1}{R_y} - \frac{1}{R_x}\right)\left(\frac{\partial v}{\partial x} - \frac{\partial u}{\partial y}\right) \qquad 3.11$$

3.5 Finite element formulations

For complex boundary and geometrical conditions where analytical approach is not so easily feasible, the finite element approach will be opted. Here, in this work the plate is assumed to be a layered panel having number of layers, in which each layer is assumed as homogenous and isotropic. The first-order shear deformation theory is used for the present formulation to analyse the FG material twisted panel.

An isoparametric quadratic shell element with eight nodes at its mid-surface shown in Figure 3. 3 is considered for the analysis. In this shell element u, v, w, θ_x and θ_y are the five degrees of freedom each node. The Jacobian matrix *J* is used to transform the isoparametric

element from the natural coordinate to the Cartesian coordinate system. The shape function for the eight noded shell element is given by,

$$u(\xi,\eta) = \alpha_1 + \alpha_2\xi + \alpha_3\eta + \alpha_4\xi^2 + \alpha_5\xi\eta + \alpha_6\eta^2 + \alpha_7\xi^2\eta + \alpha_8\xi\eta^2 \qquad 3.12$$

The shape function N_i gives the element and displacement field,

$$N_i = (1+\xi\xi_i)(1+\eta\eta_i)(\xi\xi_i + \eta\eta_i - 1)/4 \qquad \text{i=1 to 4}$$

$$N_i = (1-\xi^2)(1+\eta\eta_i)/2 \qquad \text{i= 5, 7} \qquad 3.13$$

$$N_i = (1+\xi\xi_i)(1-\eta^2)/2 \qquad \text{i=6, 8}$$

Where,

ξ_i and η_i are the values at i[th] node. ξ and η are the local natural coordinates of the element.

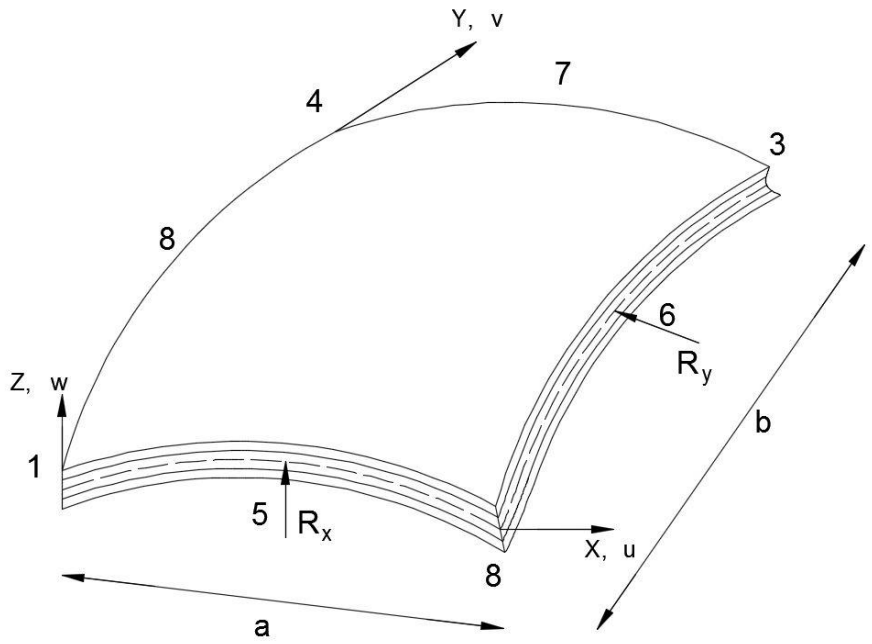

Figure 3. 3: Element of an Isoparametric quadratic shell

The shape function derivatives in Cartesian coordinates 'x' and 'y' are expressed in natural coordinates ξ and η by,

$$\begin{bmatrix} N_{i,x} \\ N_{i,y} \end{bmatrix} = [J]^{-1} \begin{bmatrix} N_{i,\xi} \\ N_{i,\eta} \end{bmatrix} \quad 3.14$$

Where,

Jacobian matrix, $|J| = \begin{bmatrix} x_{i,\xi}\ y_{i,\xi} \\ x_{i,\eta}\ y_{i,\eta} \end{bmatrix}$ 3.15

According to first order shear deformation theory, the displacement field is given by,

$$u(x,y,z) = u_0(x,y) + z\theta_y(x,y)$$

$$v(x,y,z) = u_0(x,y) + z\theta_x(x,y) \quad 3.16$$

$$w(x,y,z) = w_0(x,y)$$

Where u_0, v_0 and w_0 are the displacements in x, y and z directions respectively in the mid-plane. And u, v and w are the displacements in x, y and z directions respectively at any point.

θ_x - Rotation of the mid surface normal to x-axis.

and θ_y - rotation of the mid surface normal to y-axis.

Displacements derived using the shape functions are,

$$x = \sum N_i x_i \qquad y = \sum N_i y_i$$

$$u_0 = \sum N_i u_i \qquad v_0 = \sum N_i v_i \qquad w_0 = \sum N_i w_i \quad 3.17$$

$$\theta_x = \sum N_i \theta_{xi} \qquad \theta_y = \sum N_i \theta_{yi}$$

3.5.1 Derivation of element matrices

The linear strains expressed in terms of displacements is given by,

$$\{\varepsilon\} = [B]\{d_e\} \tag{3.18}$$

Here, $$\{d_e\} = \{u_1, v_1, w_1, \theta_{x1}, \theta_{y1}, \ldots\ldots\ldots\ldots\ldots\ldots u_8, v_8, w_8, \theta_{x8}, \theta_{y8}\} \tag{3.19}$$

$$[B] = [[B_1], [B_2], \ldots\ldots\ldots\ldots\ldots [B_8]] \tag{3.20}$$

$$[B_i] = \begin{bmatrix} N_{i,x} & 0 & \frac{N_i}{R_x} & 0 & 0 \\ 0 & N_{i,\mathrm{y}} & \frac{N_i}{R_y} & 0 & 0 \\ N_{i,\mathrm{y}} & N_{i,x} & 2\frac{N_i}{R_{xy}} & 0 & 0 \\ 0 & 0 & 0 & N_{i,x} & 0 \\ 0 & 0 & 0 & 0 & N_{i,\mathrm{y}} \\ 0 & 0 & 0 & N_{i,\mathrm{y}} & N_{i,x} \\ 0 & 0 & N_{i,x} & N_i & 0 \\ 0 & 0 & N_{i,\mathrm{y}} & 0 & N_i \end{bmatrix} \tag{3.21}$$

In natural coordinate system, element matrices are derived as:

Element plane elastic stiffness matrix

$$[k_p] = \int_{-1}^{1}\int_{-1}^{1} [B_p]^T [D_p][B_p]|J|\, d\xi d\eta \tag{3.22}$$

Element elastic stiffness matrix

$$[k_e] = \int_{-1}^{1}\int_{-1}^{1} [B]^T [D][B]|J|\, d\xi d\eta \tag{3.23}$$

Where,

$[B]$ is strain-displacement matrix, $[D]$ stress-strain matrix, $[N]$ is shape function matrix and $|J|$ is the determinant of Jacobian matrix.

Shape function matrix is expressed as:

$$[N] = I_5 \times N_i \quad \text{For i=1, 2,.....8} \tag{3.24}$$

Where, I_5 - Identity matrix of size 5x5.

3.5.2 Geometric stiffness matrix

The nonlinear strains with curvature component are used to derive the element geometric stiffness matrix for the twisted plate by employing the technique described by Cook, Malkus and Plesha [3]. Due to applied edge loading, the geometric stiffness matrix depends on in-plane stress distribution in the element. Finite element method is employed in carrying out plane stress analysis to determine the stresses.

The strain energy is given by,

$$U_2 = \int_v \left[\sigma^0\right]^T \{\varepsilon_{nl}\} dv \tag{3.25}$$

The non-linear strain components are given by,

$$\varepsilon_{xnl} = \frac{1}{2}\left(\frac{\partial u}{\partial x}\right)^2 + \frac{1}{2}\left(\frac{\partial v}{\partial x}\right)^2 - \frac{1}{2}\left(\frac{\partial w}{\partial x} - \frac{u}{R_x}\right)^2 + \frac{1}{2}z^2\left[\left(\frac{\partial \theta_x}{\partial x}\right)^2 + \left(\frac{\partial \theta_y}{\partial x}\right)^2\right] \tag{3.26}$$

$$\varepsilon_{ynl} = \frac{1}{2}\left(\frac{\partial u}{\partial y}\right)^2 + \frac{1}{2}\left(\frac{\partial v}{\partial y}\right)^2 - \frac{1}{2}\left(\frac{\partial w}{\partial y} - \frac{u}{R_y}\right)^2 + \frac{1}{2}z^2\left[\left(\frac{\partial \theta_x}{\partial y}\right)^2 + \left(\frac{\partial \theta_y}{\partial y}\right)^2\right]$$

$$\gamma_{xnl} = \frac{\partial u}{\partial x}\left(\frac{\partial u}{\partial y}\right) + \frac{\partial v}{\partial x}\left(\frac{\partial v}{\partial y}\right) + \left(\frac{\partial w}{\partial x} - \frac{u}{R_x}\right)\left(\frac{\partial w}{\partial y} - \frac{v}{R_y}\right) + z^2\left[\left(\frac{\partial \theta_x}{\partial x}\right)\left(\frac{\partial \theta_x}{\partial y}\right) + \left(\frac{\partial \theta_y}{\partial x}\right)\left(\frac{\partial \theta_y}{\partial y}\right)\right]$$

The strain energy obtained by using non-linear strain is,

$$U_2 = \int_A \frac{h}{2}\left[\begin{array}{c}\sigma_x^0\left\{\left(\frac{\partial u}{\partial x}\right)^2+\left(\frac{\partial v}{\partial x}\right)^2+\left(\frac{\partial w}{\partial x}-\frac{u}{R_x}\right)^2\right\}+\sigma_y^0\left\{\left(\frac{\partial u}{\partial y}\right)^2+\left(\frac{\partial v}{\partial y}\right)^2+\left(\frac{\partial w}{\partial y}-\frac{v}{R_y}\right)^2\right\}+\\ 2\tau_{xy}^0\left\{\left(\frac{\partial u}{\partial x}\frac{\partial u}{\partial y}\right)+\left(\frac{\partial v}{\partial x}\frac{\partial v}{\partial y}\right)+\left(\frac{\partial w}{\partial x}-\frac{u}{R_x}\right)\left(\frac{\partial w}{\partial y}-\frac{v}{R_y}\right)\right\}\end{array}\right]dxdy +$$

$$\int_A \frac{h^3}{24}\left[\sigma_x^0\left\{\left(\frac{\partial \theta_x}{\partial x}\right)^2+\left(\frac{\partial \theta_y}{\partial x}\right)^2\right\}+\sigma_y^0\left\{\left(\frac{\partial \theta_x}{\partial y}\right)^2+\left(\frac{\partial \theta_y}{\partial y}\right)^2\right\}+2\tau_{xy}^0\left\{\left(\frac{\partial \theta_y}{\partial x}\frac{\partial \theta_x}{\partial y}\right)+\left(\frac{\partial \theta_x}{\partial x}\frac{\partial \theta_y}{\partial y}\right)\right\}\right]dxdy \quad 3.27$$

This can also be written as

$$U_2 = \frac{1}{2}\int_v [f]^T [S][f]dV \quad 3.28$$

Where

$$\{f\} = \left[\frac{\partial u}{\partial x}, \frac{\partial u}{\partial y}, \frac{\partial v}{\partial x}, \frac{\partial v}{\partial y}, \left(\frac{\partial w}{\partial x}-\frac{u}{R_x}\right), \left(\frac{\partial w}{\partial y}-\frac{u}{R_y}\right), \frac{\partial \theta_x}{\partial x}, \frac{\partial \theta_x}{\partial y}, \frac{\partial \theta_y}{\partial x}, \frac{\partial \theta_y}{\partial y}\right]^T \quad 3.29$$

And, $$[S] = \begin{bmatrix}[S] & 0 & 0 & 0 & 0\\ 0 & [S] & 0 & 0 & 0\\ 0 & 0 & [S] & 0 & 0\\ 0 & 0 & 0 & [S] & 0\\ 0 & 0 & 0 & 0 & [S]\end{bmatrix} \quad 3.30$$

Where, $$[S] = \begin{bmatrix}\sigma_x^0 & \tau_{xy}^0\\ \tau_{xy}^0 & \sigma_y^0\end{bmatrix} = \frac{1}{h}\begin{bmatrix}N_x^0 & N_y^0\\ N_{xy}^0 & N_y^0\end{bmatrix} \quad 3.31$$

The in-plane stress resultants N_x^0, N_y^0 and N_{xy}^0 each Gauss point are obtained separately by plane stress analysis, and the geometric stiffness matrix is formed for these stress resultants

$$\{f\} = [G]\{q_e\} \quad 3.32$$

Where, $$\{q_e\} = \begin{bmatrix}u & v & w & \theta_x & \theta_y\end{bmatrix}^T \quad 3.33$$

The strain energy becomes

$$U_2 = \frac{1}{2}\{q\}^T [G]^T [S][G]\{q\} dV = \frac{1}{2}\{q_e\}^T \left[K_g\right]_e [q_e] \tag{3.34}$$

Where the element geometric stiffness matrix is expressed as:

$$\left[k_g\right]_e = \int_{-1}^{1}\int_{-1}^{1} [G]^T [S][G]|J| d\xi d\eta \tag{3.35}$$

$$[G] = \begin{bmatrix} N_{i,}x & 0 & 0 & 0 & 0 \\ N_{i,}y & 0 & 0 & 0 & 0 \\ 0 & N_{i,}x & 0 & 0 & 0 \\ 0 & N_{i,}y & 0 & 0 & 0 \\ 0 & 0 & N_{i,}x & 0 & 0 \\ 0 & 0 & N_{i,}y & 0 & 0 \\ 0 & 0 & 0 & N_{i,}x & 0 \\ 0 & 0 & 0 & N_{i,}y & 0 \\ 0 & 0 & 0 & 0 & N_{i,}x \\ 0 & 0 & 0 & 0 & N_{i,}y \end{bmatrix} \tag{3.36}$$

3.6 Methodology

This project work involves creating a finite element model of a functionally graded twisted plate subjected to in-plane uniform compressive load. The initial step is to build a model of a functionally graded plate using ANSYS. First a flat FGM plate will be modelled, and buckling behavior will be analyzed, and the results are compared with previous studies. Then a twisted functionally graded plate will be modelled and analyzed for its characteristics subjected to in-plane loads. Results will be analyzed and validated with the calculations using ABAQUS.

The three steps involved in modelling and analysis of plates are:

I. Pre- Processor

II. Solution

III. General Postprocessor

3.6.1 Material modelling

FGMs consist of a mixture of metal and ceramic by gradually varying the volume fraction of the constituent materials. A simple rule of mixture based on power-law is assumed to obtain the effective mechanical properties of FGM plate. The variation of material properties through the thickness of the plate is given by (Reddy, 2000) [14]

$$P_z = (P_t - P_b)V_f + P_b \qquad 3.37$$

where subscripts *t* and *b* refers to the top and bottom of the plate respectively, P_z represents a property of the material and *z* is measured along the thickness of the plate. In Eq.(3.37), V_f is the volume content of ceramic and is expressed by power-law distribution as

$$V_f = \left(\frac{z}{h} + 0.5\right)^n \qquad 3.38$$

In which h is the thickness of the plate. n is the gradient index that is always positive, and z is the distance from the centre of layer under consideration to the centre of plate in which $-(h/2) \leq z \leq +(h/2)$. Change of V_f over plate thickness is shown in Figure 3. 4.

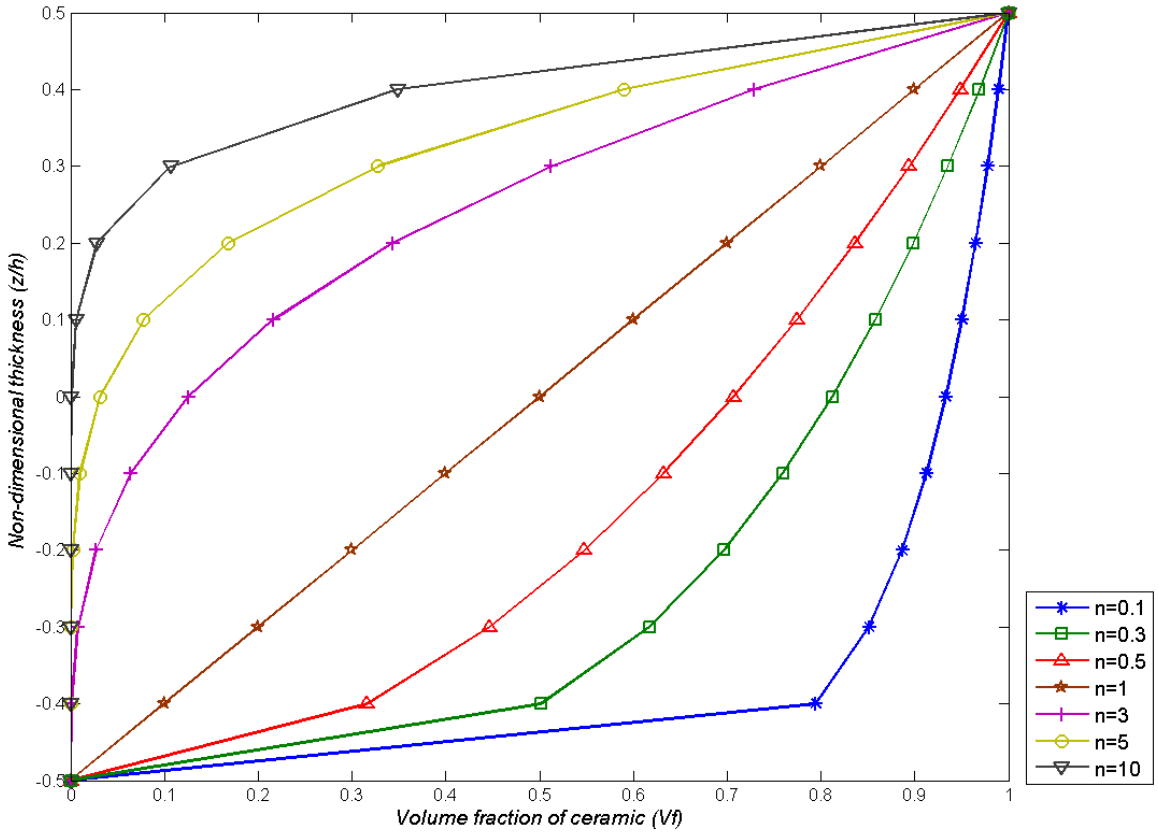

Figure 3. 4: Change of Volume fraction (Vf) over plate thickness

Since the material constituents of the FG material varies over the thickness, the numerical model is made into divisions consisting of a number of layers as shown in Figure 3. 5. Each layer is assumed to be isotropic. The power law is employed to find the material properties in each

layer. The laminated structure represents the stepwise variation in properties, and the gradation can be approximated by using a high number of layers.

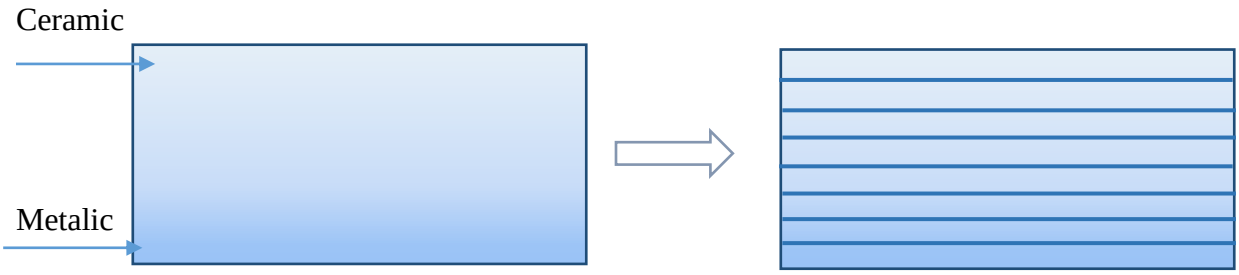

Figure 3. 5: FG Material section and its equivalent laminated composite section

Chapter 4

RESULTS AND DISCUSSIONS

CHAPTER 4

RESULTS AND DISCUSSIONS

4.1 Overview

In this section, the results of the buckling analysis of cantilever twisted functionally graded material plates subjected to in-plane loads are presented. The analysis is carried out using finite element software ANSYS with the SHELL281 element. The element considered has eight nodes and each node has six degrees of freedom. The functionally graded material plate section is modelled in the form of laminated composite section consisting of number of layers by approximating the uniform variation of the material property along the thickness and considering each layer as isotropic. The power law is used to determine the material properties of each layer. Convergence studies are made to fix up the number of layers and mesh size as well, and results are compared with the previous studies.

4.2 Convergence study

The convergence study is made for the mesh size necessary for the buckling analysis and also for the number of layers necessary to represent the FG material section. Since there are no studies done on twisted FGM plates, the convergence is first conducted on flat plates, and the results are compared with previous studies. Later the convergence is made on twisted FGM plate and then mesh size, and number of layers is again decided.

The Aluminium/Alumina *(Al/Al_2O_3)* FGM [15] with the material properties *Al* - (E_m = 70GPa, υ = 0.3), Al_2O_3 - (E_c = 380GPa, υ = 0.3) are considered for the present study throughout.

The Titanium/Zirconium oxide *(Ti/ZrO_2)* FGM [5] with the material properties *Ti* – (E_m=116GPa, υ = 0.32) and *ZrO_2* – (E_c = 200GPa, υ = 0.3) are used in finding the buckling behavior for varying gradient index.

Non-dimensional buckling load is given by [15]

$$\lambda = \frac{N_x b^2}{E_m h^3}$$

4.2.1 Convergence study on simply supported flat FGM plate

The convergence study on simply supported flat FGM plate with gradient index n = 0 for various mesh divisions are shown in Table 4. 1. The results show good convergence for 10×10 mesh division and hence, the 10×10 mesh division is used for the further study.

Table 4. 1: Convergence of Non- dimensional buckling load of simply supported flat FGM plate (n=0) with varying mesh size (a/b =1, b/h=100)

Mesh size	**Buckling Load (N_x) kN**	**Non-dimensional Buckling Load (λ)**
4×4	696.59	19.9025
6×6	687.00	19.6285
8×8	686.59	19.6168
10×10	686.53	19.6151
12×12	686.52	19.6148
Ref [20]		19.57

FGM section is considered as an equivalent laminate section for the modelling. The convergence study is done by using simply supported flat FGM plate with varying number of layers using gradient index n = 1. The observations are given in Table 4. 2. From the observations, it is concluded that the 12 number of layers are sufficient to represent FGM property as an equivalent laminate section.

Table 4. 2: Convergence of Non- dimensional buckling load of simply supported flat FGM plate (n=1) with varying number of layers (a/b =1, b/h=100)

Number of Layers	Buckling Load (N_x) kN	Non-dimensional Buckling Load (λ)
4	350.01	10.0002
8	344.23	9.8351
12	343.12	9.8034
16	342.73	9.7922
Ref [15]		9.7775

4.2.2 Convergence study on Cantilever twisted FGM plate

The convergence study on cantilever twisted FGM plate with gradient index n = 0, and twist angle Φ =15° for various mesh divisions is shown in Table 4. 3. The results show good convergence for 10×10 mesh division and the same is used for the further study.

Table 4. 3: Convergence results of Non- dimensional buckling load of cantilever twisted FGM plate (n= 0) with varying mesh size (a/b =1, b/h=100, Φ =15°)

Mesh size	Buckling Load (N_x) kN		Non-dimensional Buckling Load (λ)	
	1st Buckling	2nd Buckling	1st Buckling	2nd Buckling
4×4	41.300	365.17	1.1800	10.4334
6×6	41.197	362.86	1.1771	10.3674
8×8	41.172	362.35	1.1763	10.3528
10×10	41.163	362.19	1.1761	10.3483
12×12	41.160	362.13	1.1760	10.3465

Convergence study for the number layers on cantilever twisted FGM plate with gradient index n = 1 is shown in Table 4. 4. From the observations, it is concluded that 12 number of layers are sufficient to represent FGM property as equivalent laminate section, hence 12 number of layers are used in the further studies.

Table 4. 4: Convergence results of Non- dimensional buckling load of cantilever twisted FGM plate (n=1) with varying number of layers (a/b =1, b/h=100, Φ =15°)

Number of layers	Buckling Load (N_x) kN		Non-dimensional Buckling Load (λ)	
	1st Buckling	2nd Buckling	1st Buckling	2nd Buckling
4	20.998	184.79	0.5999	5.2797
8	20.652	181.75	0.5901	5.1928
12	20.586	181.17	0.5882	5.1763
16	20.563	180.96	0.5875	5.1703

4.3 Comparison with previous studies

The comparative studies are made on cantilever twisted laminated panels to validate the methodology used in ANSYS. The results obtained are closely matched with the previous study results. Table 4. 5 and Table 4. 6 shows the comparative study on the variation of Non-dimensional buckling load of cantilever twisted laminated panels with different angle of twist and aspect ratio respectively.

Table 4. 5: Comparative study of the variation of Non-dimensional buckling load of cantilever twisted laminated panels for different angle of twist (Φ)

(a/b=1, b/h=250, E_{11}=141GPa, E_{22}=9.23GPa, υ_{12}=0.313, G_{12}=5.95GPa, G_{23}=2.96GPa)

Angle of Twist Φ	Non-dimensional Buckling Load (λ)			
	Present		Ref [1]	
	0°/90°	0°/90°/0°/90°	0°/90°	0°/90°/0°/90°
0°	0.7106	1.4397	0.7106	1.4432
10°	0.7000	1.4191	0.6949	1.4078
20°	0.6698	1.3570	0.6473	1.3114
30°	0.6202	1.2556	0.5689	1.1526

Table 4. 6: Comparison study of the variation of Non-dimensional buckling load of cantilever twisted laminated panels for different aspect ratio (a/b) (Φ =15°, b/h=250)

a/b	Non-dimensional Buckling Load (λ)			
	Present		Ref [1]	
	0°/90°	0°/90°/0°/90°	0°/90°	0°/90°/0°/90°
0.5	2.7050	5.4780	2.7010	5.4706
1	0.6876	1.3931	0.6750	1.3676
2	0.1725	0.3496	0.1687	0.3418
3	0.0767	0.1555	0.0750	0.1519

In both cases, the results agree very well. Hence, the twisted plate modelling in ANSYS gives good results.

4.4 Results and Discussions

Buckling analysis of cantilever twisted Aluminium/Aluminium oxide (Al/Al_2O_3) FG material plate is studied. The material properties are *Al* - (E_m = 70GPa, υ = 0.3), Al/Al_2O_3 - (E_c = 380GPa, υ = 0.3). The effect of various parameters on the buckling of pre-twisted FGM plate is studied.

Non-dimensional buckling load is given by

$$\lambda = \frac{N_x b^2}{E_m h^3}$$

The non-dimensional buckling load for the cantilever twisted plate with varying twist angle is studied first using ANSYS and then the results obtained in ANSYS are validated using ABAQUS. The results obtained are shown in Table 4. 7, and the same is shown graphically for the first buckling mode in Figure 4. 1. The results obtained in ANSYS and ABAQUS are close to

each other and hence, further studies are continued with ANSYS. From the results, it is observed that the Non-dimensional buckling load decreases with increase in twist angle.

Table 4. 7: Variation of Non-dimensional buckling load with varying twist angle (Φ) (a/b=1, b/h=100, n=1)

Angle of Twist	Non-dimensional Buckling Load (λ)			
	ANSYS		ABAQUS	
	1st Buckling mode	2nd Buckling mode	1st Buckling mode	2nd Buckling mode
0°	0.5899	4.4685	0.5924	4.5566
10°	0.5896	5.2485	0.5918	5.4408
15°	0.5882	5.1763	0.5902	5.3657
20°	0.5852	5.0657	0.5872	5.2514
30°	0.5758	4.7497	0.5775	4.9237

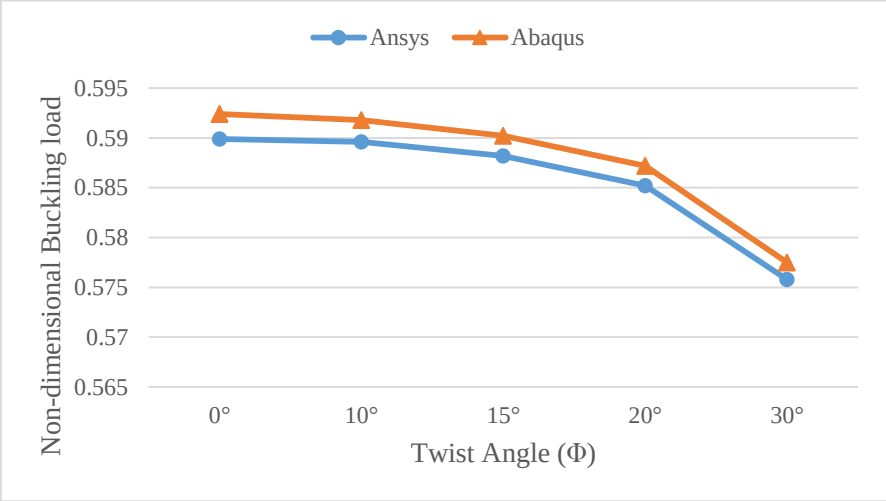

Figure 4. 1: Variation of Non-dimensional buckling load with varying twist angle (Φ)

The 1st and 2nd buckling modes of untwisted and 15° twisted plates are shown in the Figure 4. 2 and Figure 4. 3 respectively.

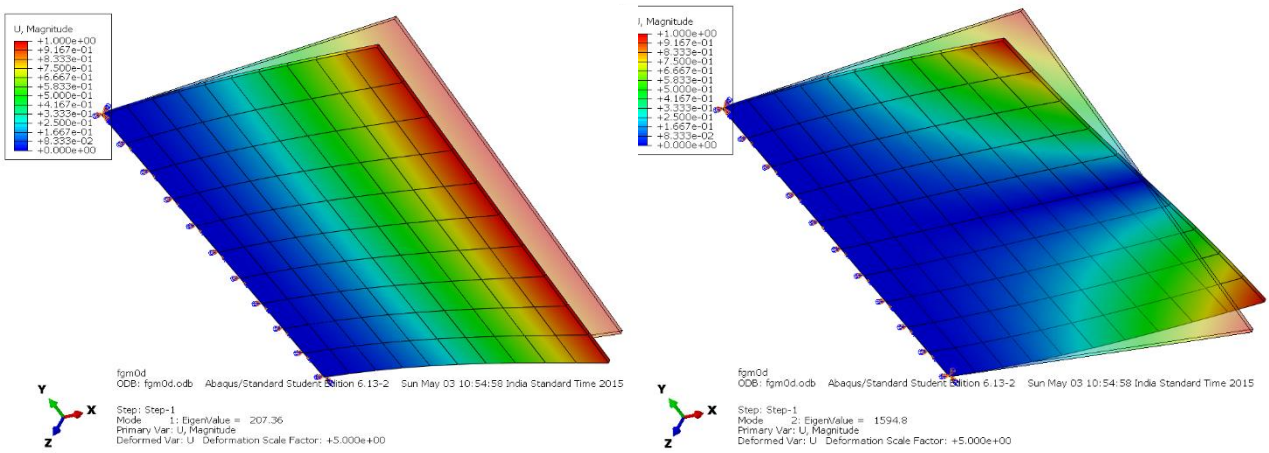

1st Mode 2nd Mode

Figure 4. 2: Buckling modes of an untwisted plate

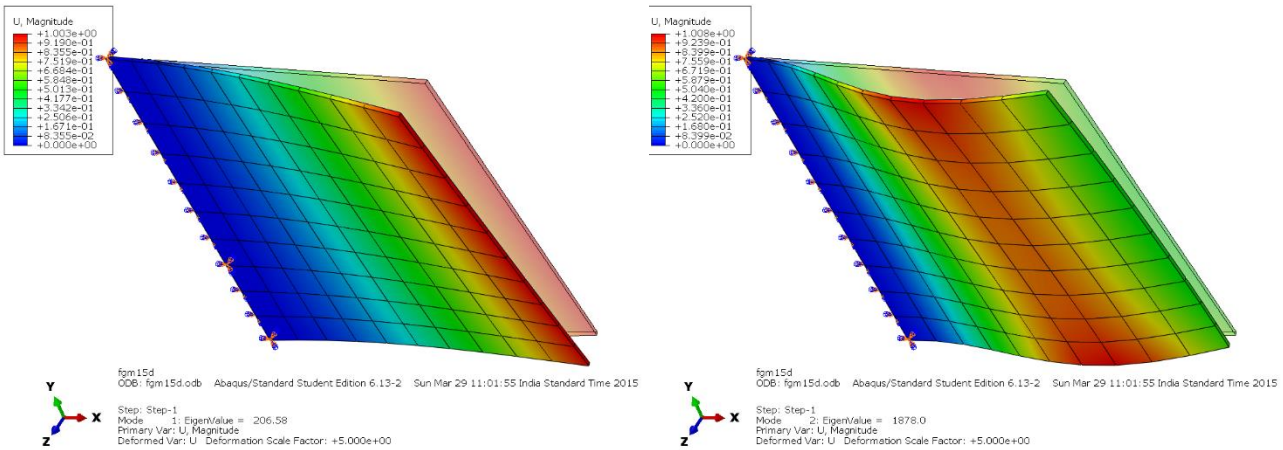

1st mode 2nd mode

Figure 4. 3: Buckling modes of 15° twisted plate.

Variation of non-dimensional buckling load with increasing aspect ratio for different gradient index n = 1 and n = 2 is then studied with twist angle 15° and results are presented in Table 4. 8 and Table 4. 9 respectively. The variation of non-dimensional buckling load is shown graphically in the Figure 4. 4. From the results, it has been observed that the non-dimensional buckling load decreases largely with increasing aspect ratio. This is because when the aspect ratio increases, the length of the plate in the direction of the in-plane compression load acting also increases resulting in decreased stiffness. Hence, the amount of critical buckling load required to cause critical buckling decreases.

Table 4. 8: Variation of Non-dimensional buckling load with varying aspect ratio (a/b) (b/h=100, Φ =15°, n=1)

a/b	**Non-dimensional Buckling Load (λ)**	
	1st Buckling	**2nd Buckling**
0.5	2.4338	17.4845
1	0.5882	5.1766
2	0.1443	1.2734
3	0.0634	0.5606

Table 4. 9: Variation of Non-dimensional buckling load with varying aspect ratio (a/b) (b/h=100, Φ =15°, n=2)

a/b	**Non-dimensional Buckling Load (λ)**	
	1st Buckling mode	**2nd Buckling mode**
0.5	1.8321	13.5971
1	0.4589	4.0383
2	0.1125	0.9936
3	0.0495	0.4374

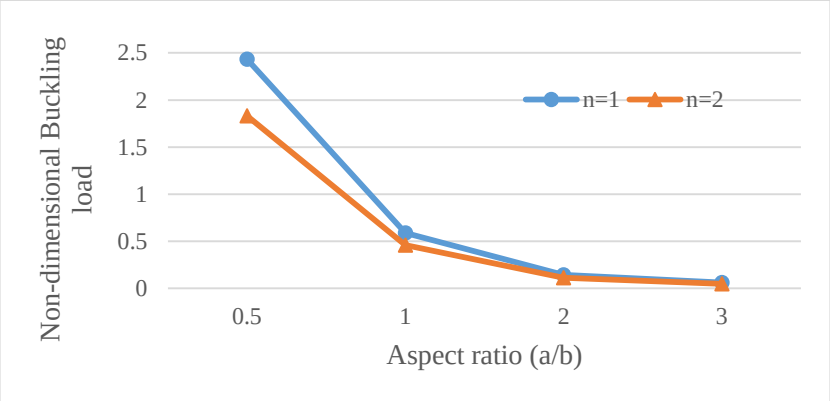

Figure 4. 4: Variation of Non-dimensional buckling load with varying aspect ratio(a/b)

The variation of non-dimensional buckling load with increasing side to thickness ratio for a 15° pre-twisted plate is studied, and the results obtained are presented in Table 4. 10 and the graphical representation of variation is shown in Figure 4. 5. From the results, it has been observed that the critical buckling load decreases with increasing the side to thickness ratio but the non-dimensional buckling load increases with increasing the side to thickness ratio. Because, as the side to thickness ratio of twisted plate increases, the stiffness of the plate decreases, and thus it decreases the critical buckling load. But in Non-dimensional buckling load, the term 'h' is in the denominator and hence it shows increasing value with increasing the side to thickness ratio.

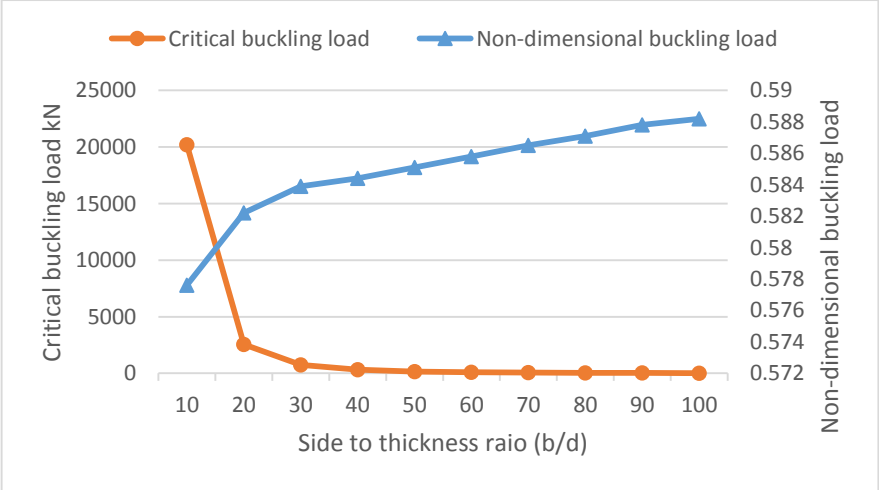

Figure 4. 5: Variation of non-dimensional buckling load with varying side to thickness ratio(b/d)

Table 4. 10: Variation of Non-dimensional buckling load with varying side to thickness ratio(b/d) (a/b=1, Φ =15°, n=1)

b/h	Buckling Load (N_x) kN		Non-dimensional Buckling Load (λ)	
	1st Buckling	2nd Buckling	1st Buckling	2nd Buckling
10	20218	156470	0.5776	4.4706
20	2547.10	22144	0.5822	5.0615
30	756.91	6622.20	0.5839	5.1085
40	319.60	2802.80	0.5844	5.1251
50	163.84	1438.60	0.5851	5.1378
60	94.925	834.14	0.5858	5.1478
70	59.844	526.15	0.5865	5.1563
80	40.132	352.99	0.5871	5.1637
90	28.220	248.29	0.5878	5.1715
100	20.586	181.17	0.5882	5.1763

The variation of non-dimensional buckling load with increasing gradient index for a 15° pre-twisted plate is studied for two different FGMs Al/Al_2O_3 and Ti/ZrO_2. The results obtained are presented in Table 4. 11 and Table 4. 12. From the results, it is observed that non-dimensional buckling load decreases with increase in the gradient index. This is because, when the gradient index is zero, the plate will be completely ceramic which is very stiff and hence the critical buckling load is higher. As it goes on increasing, the metal content in the plate also increases, resulting in reduced stiffness and, therefore, the critical buckling load goes on decreasing. When the gradient index reaches infinity, the plate will be completely metallic which is less stiff than ceramic and thus critical buckling load is less. The variation is shown in the Figure 4. 6 and Figure 4. 7.

Table 4. 11: Variation of Non-dimensional buckling load with varying gradient index (n) for Al/Al2O3 FGM (a/b=1, Φ =15°, b/h=100)

Gradient index (n)	Buckling Load (N_x) kN		Non-dimensional Buckling Load (N_x)	
	1st Buckling	2nd Buckling	1st Buckling	2nd Buckling
0 (Al_2O_3)	41.163	362.19	1.1761	10.3483
0.5	26.270	231.42	0.7506	6.6120
1	20.586	181.17	0.5882	5.1763
2	16.062	141.34	0.4589	4.0383
5	13.510	118.85	0.3860	3.3957
10	12.386	108.95	0.3539	3.1128
20	12.298	99.377	0.3228	2.8393
30	10.865	95.571	0.3104	2.7306
50	10.615	93.374	0.3033	2.6678
100	10.563	92.918	0.3018	2.6548
∞ (*Al*)	7.5827	66.720	0.2166	1.9063

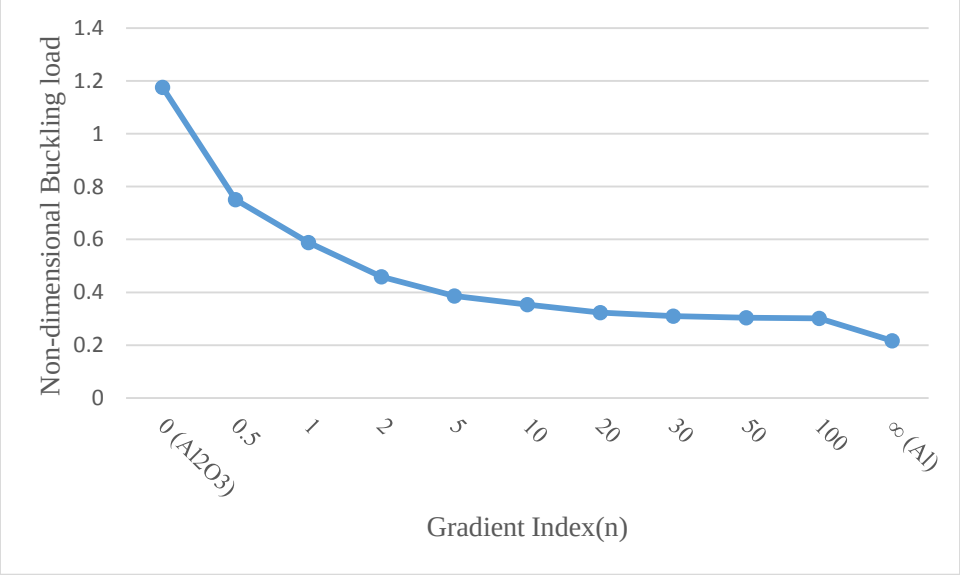

Figure 4. 6: Variation of Non-dimensional buckling load with varying gradient index(n) for Al/Al2O3 FGM.

Table 4. 12: Variation of Non-dimensional buckling load with varying gradient index (n) for Ti/ZrO2 FGM (a/b=1, Φ =15°, b/h=100)

Gradient index (n)	Buckling Load (N_x) kN		Non-dimensional Buckling Load (N_x)	
	1st Buckling	2nd Buckling	1st Buckling	2nd Buckling
0 (CrO_2)	21.665	190.63	0.3735	3.2867
0.5	18.031	158.52	0.3109	2.7331
1	16.791	147.74	0.2895	2.5472
2	15.811	139.12	0.2726	2.3986
5	14.943	131.46	0.2576	2.2665
10	14.308	125.88	0.2467	2.1703
20	13.799	121.41	0.2379	2.0933
30	13.624	119.87	0.2349	2.0667
50	13.528	119.02	0.2332	2.0521
100	13.509	118.85	0.2329	2.0491
∞ (*Ti*)	12.667	111.53	0.2184	1.9229

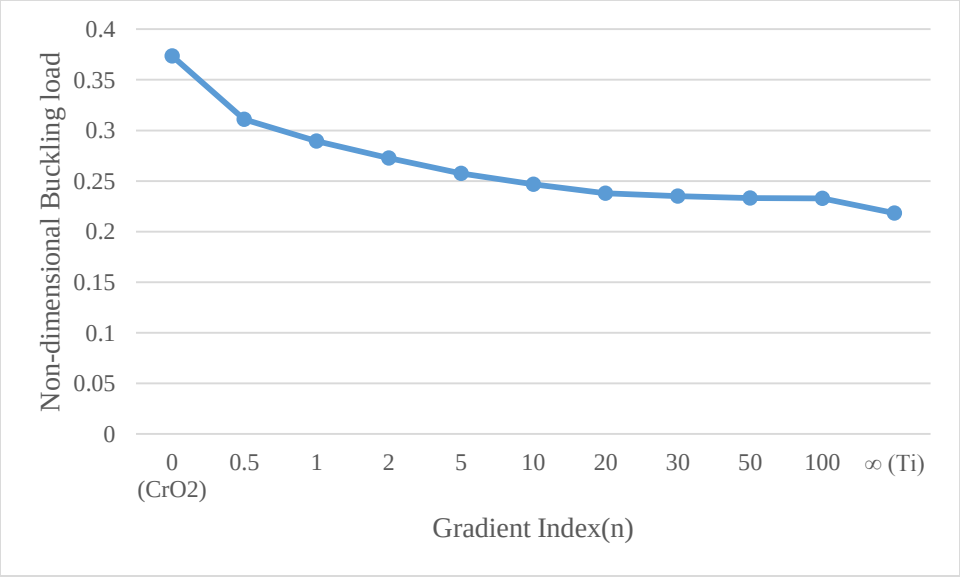

Figure 4. 7: Variation of Non-dimensional buckling load with varying gradient index (n) for Ti/ZrO2 FGM.

Chapter 5

CONCLUSIONS

CHAPTER 5

CONCLUSIONS

5.1 Conclusions

The present work enables to arrive at the following important conclusions:

- With the increase in angle of twist, the non-dimensional buckling load decreases.
- As the aspect ratio (a/b) increases, the non-dimensional buckling load of a twisted FGM plate decreases largely. This is because when the aspect ratio increases, the length of the plate in the direction of the in-plane compression load also increases resulting in the decreased stiffness. Hence, the amount of critical buckling load required to cause critical buckling decreases.
- The non-dimensional buckling load also increases with increase in the side to thickness ratio (b/d). Because, as the side to thickness ratio of the twisted plate increases, the stiffness of the plate decreases as well, and thus it increases critical buckling load.
- The non-dimensional buckling load decreases with increase in the material index of a pre-twisted functionally graded material plate. This is because, as the material gradient goes on increasing, the metal content in the plate also increases but the ceramic content decreases resulting in reduced stiffness and, therefore, the critical buckling load goes on decreasing with increase in gradient index.

5.2 Scope of Future Works

The present study can be extend to:

- Study the effect of thermal loads alone and combination of mechanical and thermal loads on the buckling analysis of twisted FG material plate.
- Considering different varying edge load on buckling analysis of twisted functionally graded material plate.
- Study the non-linear buckling analysis of twisted functionally graded material plate.

REFERENCES

1. Asha. A. V, Shishir Kumar Sahu, Parametric instability of twisted cross-ply laminated panels, *Aerospace Science and Technology*, vol. 15, pp. 465–475, 2011.
2. Ashraf M.Zenkour, Daoud S. Mashat, Thermal buckling analysis of ceramic-metal functionally graded plates, *Natural Science*, vol.2, No.9, pp. 968-978, 2010.
3. Cook, R, Malkus, D.S. and Plesha, M. E, Concepts and Applications of Finite Element, *Analysis, John Wiley & Sons, U.S.A.* 1989.
4. Chandrashekhara. K, Free vibrations of anisotropic laminated doubly curved shells, *Computers and Structures*, vol.33 (2), 435-440, 1989.
5. Hideaki Tsukamoto, Mechanical Properties of Zirconia-Titanium Composites. *International Journal of Materials Science and Applications*.Vol. 3, No. 5, pp. 260-267, 2014.
6. Javaheri R, Eslami MR, Thermal buckling of functionally graded plates based on higher order theory, *J. Thermal Stresses*, vol. 25, pp. 603–25, 2002.
7. Mahadavian. M, Buckling Analysis of Simply-supported Functionally Graded Rectangular Plates under Non-uniform In-plane Compressive Loading, *Journal of Solid Mechanics*, vol. 1, No. 3, pp. 213-225, 2009.
8. Manish Bhandari, Kamlesh Purohit, Analysis of Functionally Graded Material Plate under Transverse Load for Various Boundary Conditions, *IOSR Journal of Mechanical and Civil Engineering,* e-ISSN: 2278-1684,p-ISSN: 2320-334X, vol. 10, Issue 5, pp. 46-55, 2014.

9. Matin Latifi, Fatemeh Farhatnia, Mahmoud Kadkhodaei, Buckling analysis of rectangular functionally graded plates under various edge conditions using Fourier series expansion, *European Journal of Mechanics A/Solids*, vol. 41, pp. 16-27, 2013.
10. Meisam Mohammadi, Ali Reza Saidi, Emad Jomehzadeh, Levy Solution for Buckling Analysis of Functionally Graded Rectangular Plates, *Appl Compos Mater*, vol. 17, pp. 81–93, 2010.
11. Mostapha Raki, Reza Alipour and Amirabbas Kamanbedast, Thermal Buckling of Thin Rectangular FGM Plate, *World Applied Sciences Journal*, vol. 16 (1), pp. 52-62, 2012.
12. Naderi. A, Saidi. A. R, Exact solution for stability analysis of moderately thick functionally graded sector plates on elastic foundation, *Composite Structures,* vol. 93, pp. 629–638, 2011.
13. Prakash. T, Singha. M.K, Ganapathi. M, Thermal post buckling analysis of FGM skew plates, *Engineering Structures*, vol. 30, pp. 22–32, 2008.
14. Reddy. J. N, Analysis of functionally graded plates, *Int. J. Numer. Meth. Engng.*, Vol. 47, pp. 663-684, 2000.
15. Rohit Saha, Maiti. P. R, Buckling of simply supported FGM plates under uniaxial load, *International Journal of Civil and Structural Engineering*, Volume 2, No 4, 2012.
16. Sahu. S.K and Datta. P.K, Dynamic stability of laminated composite curved panels with cutouts, *Journal of Engineering Mechanics*, ASCE, vol. 129(11), 1245-1253, 2003.
17. Samsam Shariat. B. A, Javaheri. R, Eslami. M. R, Buckling of imperfect functionally graded plates under in-plane compressive loading, *Thin-Walled Structures*, vol. 43, pp. 1020–1036, 2005.

18. Samsam Shariat. B. A, Eslami. M. R, Buckling of thick functionally graded plates under mechanical and thermal loads, *Composite Structures,* vol. 78, pp. 433–439, 2007.
19. Sarrami-Foroushani. S, Azhari. M, Saadatpour. M.M, buckling of functionally graded stiffened and unstiffened plates using finite strip method, *Comp. Meth. Civil Eng.*, Vol.4 No.1, pp.1-24, 2013.
20. Sidda Reddy, Suresh Kumar. J, Eswara Reddy. C and Vijaya Kumar Reddy. K, Buckling Analysis of Functionally Graded Material Plates Using Higher Order Shear Deformation Theory, *Journal of Composites*, Volume 2013, Article ID 808764, 12 pages.
21. Yang. J, Liew. K. M, Kitipornchai. S, Imperfection sensitivity of the post-buckling behaviour of higher-order shear deformable functionally graded plates, *International Journal of Solids and Structures,* vol. 43, pp. 5247–5266, 2006.
22. Zhang. L.W, Zhu. P, Liew. K.M, Thermal buckling of functionally graded plates using a local Kriging meshless method, *Composite Structures*, vol. 108, pp. 472-492, 2014.
23. Zhao. X, Lee. Y.Y, Liew. K.M, Mechanical and thermal buckling analysis of functionally graded plates, *Composite Structures,* vol. 90, pp. 161–171, 2009.
24. Zenkour. A. M, Sobhy. M, Thermal buckling of various types of FGM sandwich plates, *Composite Structures,* vol. 93, no.1, pp. 93–102, 2010.